Mechanics of buckled carbon nanotubes on elastomeric substrates

J. Xiao,[1] H. Jiang,[2] D.–Y. Khang,[3] J. Wu,[4] Y. Huang,[1,5,a)] and J. A. Rogers[6]

[1]*Department of Mechanical Engineering, Northwestern University, Evanston, Illinois 60208, USA*
[2]*Department of Mechanical and Aerospace Engineering, Arizona State University, Tempe, Arizona 85287, USA*
[3]*School of Chemical and Biological Engineering, Seoul National University, Seoul 151-742, Republic of Korea*
[4]*Department of Engineering Mechanics, Tsinghua University, Beijing 100084, People's Republic of China*
[5]*Department of Civil and Environmental Engineering, Northwestern University, Evanston, Illinois 60208, USA*
[6]*Department of Materials Science and Engineering, Beckman Institute, and Seitz Materials Research Laboratory, University of Illinois at Urbana-Champaign, Illinois 61801, USA*

The buckling of carbon nanotubes (CNTs) on elastomeric substrates is studied in this paper. Simple expressions of the buckle wavelength and amplitude and the critical strain for buckling are obtained analytically. For single-walled CNTs, the wavelength is proportional to the CNT radius to the 3/4 power, while it increases linearly with the number of walls for multiwalled CNTs. For two parallel CNTs on the surface of the elastomeric substrate, there exists a critical spacing below which the two CNTs interact and buckle together, adopting the same wavelength. This cobuckling wavelength is very close to the wavelength for the larger CNT to buckle independently, i.e., the larger tube dominates the coupled buckling. © *2008 American Institute of Physics*. [DOI: 10.1063/1.2968228]

I. INTRODUCTION

Buckling of thin stiff films on an elastomeric substrate has many important applications such as stretchable electronics[1–6] and precision metrology.[7,8] Carbon nanotubes (CNTs) have superior mechanical and electrical properties[9–21] and are candidates for the next generation of electronic systems.[22–24] Buckling of CNTs on elastomeric substrates has many potential applications in stretchable electronics and, separately, as a means to perform accurate measurements of the mechanical moduli.[24,25]

Khang *et al.*[25] recently studied the buckling behavior of aligned single-walled CNTs on the poly(dimethylsiloxane) (PDMS) substrate. Arrays of aligned single-walled CNTs were first grown on a quartz substrate [Fig. 1(a)] and then transferred to a prestrained PDMS substrate [Fig. 1(b)]. Release of prestrain created buckled single-walled CNTs on the PDMS substrate [Fig. 1(c)]. Figure 1(d) shows an atomic force microscopy (AFM) image of buckled single-walled CNTs on the surface of the PDMS.

The purpose of this paper is to establish a mechanics theory for the buckling of CNTs on the elastomeric substrate. The theory includes the individual buckling of CNT as well as the coupled buckling when two CNTs interact. The theory holds for single- and multiwalled CNTs as well as CNT bundles. Simple analytical expressions of the buckle wavelength and amplitude are obtained, which agree well with experiments.

II. BUCKLING OF SINGLE-WALLED CNTS

Let R, $E_{CNT}I$, and $E_{CNT}A$ denote the radius, bending stiffness, and tensile stiffness of a CNT, respectively. The out-of-plane displacement of the buckled CNT shown in Fig. 1 can be written as $w = w_{max} \cos kx$, where x is along the tube direction, the amplitude w_{max} and wave number k are to be determined, and the wavelength $\lambda = 2\pi/k$. The bending energy (per unit length) in the CNT is

$$U_b = \frac{1}{\lambda} \int_0^\lambda \frac{1}{2} E_{CNT} I (w'')^2 dx = \frac{E_{CNT}I}{4} k^4 w_{max}^2. \qquad (1)$$

The membrane strain ε in the CNT is related to w and in-plane displacement u by $\varepsilon = u' + (w')^2/2$. Since Young's modulus E_{PDMS} of PDMS substrate (~ 1 MPa) is much smaller than the CNT modulus (~ 1 TPa), the shear stress between the CNT and substrate is negligible,[26] which leads to a constant membrane force (and therefore, constant membrane strain). This gives $u = (1/8)kw_{max}^2 \sin(2kx) - \varepsilon_{pre}x$ and the membrane strain $\varepsilon = (1/4)k^2 w_{max}^2 - \varepsilon_{pre}$, where $-\varepsilon_{pre}$ is the compressive strain due to the relaxation of prestrain ε_{pre} in the substrate. The membrane energy (per unit length) in the CNT is

$$U_m = \frac{1}{2} E_{CNT} A \varepsilon^2 = \frac{1}{2} E_{CNT} A \left(\frac{1}{4} k^2 w_{max}^2 - \varepsilon_{pre} \right)^2. \qquad (2)$$

The lateral force (per unit length) on the CNT, which is used to calculate the strain energy in the substrate, is obtained from the beam theory[27] as $T_3 = E_{CNT}Iw'''' - (E_{CNT}A\varepsilon w')' = -P \cos kx$, where $P = E_{CNT}Ak^2 w_{max}(\varepsilon_{pre} - k^2 w_{max}^2/4) - E_{CNT}Ik^4 w_{max}$.

The PDMS substrate is considered as a semi-infinite solid since its thickness is many orders of magnitude larger than the CNT buckle wavelength. The substrate surface is traction-free except for the part underneath the CNT, which has the width of CNT diameter $2R$. The normal stress traction in this region is the average of lateral force $P \cos kx$

---

a)Author to whom correspondence should be addressed. Electronic mail: y-huang@northwestern.edu.
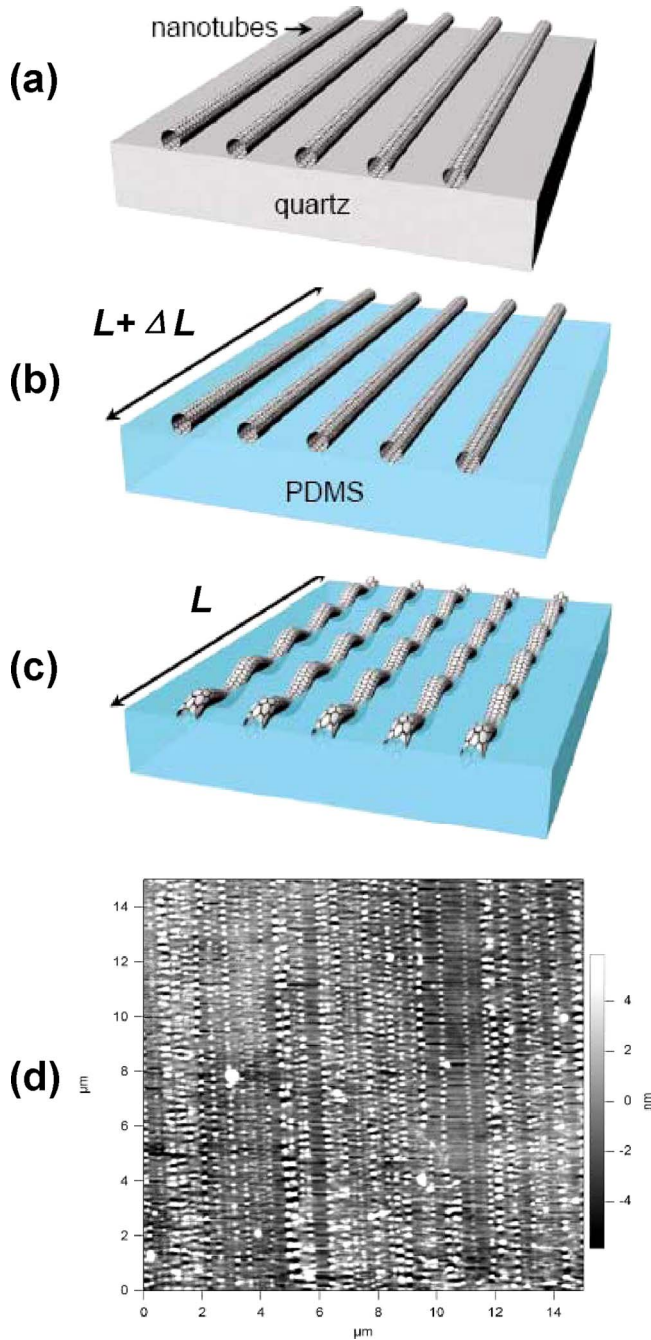
FIG. 1. (Color online) The process of forming buckled, wavy single-walled CNTs on PDMS substrate. (a) Arrays of aligned single-walled CNTs were grown on quartz substrate. (b) CNTs were transferred to a prestrained PDMS substrate; L is the original length of PDMS and ΔL is the extension. (c) Release of prestrain creates the buckled, wavy single-walled CNTs on the PDMS substrate. (d) AFM image of the buckled, wavy single-walled CNTs on the PDMS substrate using the procedure described above.

over the width, i.e., $P \cos kx/(2R)$. The Green's function for a unit normal point force at $(t_1, t_2, 0)$ on the surface of a semi-infinite solid gives the normal displacement at $(x_1, x_2, 0)$ on the surface as $[(x_1 - t_1)^2 + (x_2 - t_2)^2]^{-1/2}/(\pi \bar{E}_{\mathrm{PDMS}})$,[28] where $\bar{E}_{\mathrm{PDMS}} = 4E_{\mathrm{PDMS}}/3$ is the plane-strain modulus of the substrate since PDMS is nearly incompressible.[29] The normal displacement on the surface for the normal stress traction $P \cos kx/(2R)$ over the width $2R$ can be obtained by integrating the Green function as

$$w = \frac{P}{\pi R \bar{E}_{\mathrm{PDMS}}} \int_{-R}^{R} K_0(k|x_2 - t_2|) dt_2 \cos kx_1, \qquad (3)$$

where $K_0(k|x_2 - t_2|)$ is the modified Bessel function of the second kind. For a wavelength (~ 150 nm) much larger than the CNT radius (~ 1 nm), i.e., $kR \ll 1$, the leading term in the Taylor series expansion in Eq. (3) is

$$w = \frac{P \cos(kx_1)}{\pi R \bar{E}_{\mathrm{PDMS}}} [2R(1 - \gamma + \ln 2) - (R + x_2)\ln(k|R + x_2|)$$
$$- (R - x_2)\ln(k|R - x_2|)], \qquad (4)$$

where $\gamma = 0.577$ is the Euler constant. The strain energy in the substrate (per unit length) can be obtained in terms of the normal stress traction $P \cos kx/(2R)$ and surface displacement in Eq. (4) via the divergence theorem as

$$U_{\mathrm{PDMS}} = \frac{P^2(3 - 2\gamma - 2 \ln kR)}{4\pi \bar{E}_{\mathrm{PDMS}}}. \qquad (5)$$

The total potential energy Π_{tot} of the system is

$$\Pi_{\mathrm{tot}} = U_b + U_m + U_{\mathrm{PDMS}} - \frac{1}{\lambda} \int_0^\lambda P \cos kx(w$$
$$- w_{\mathrm{max}} \cos kx) dx = \frac{E_{\mathrm{CNT}}I}{4} k^4 w_{\mathrm{max}}^2$$
$$+ \frac{E_{\mathrm{CNT}}A}{2} \left(\frac{k^2 w_{\mathrm{max}}^2}{4} - \varepsilon_{\mathrm{pre}} \right)^2 + \frac{1}{2} P w_{\mathrm{max}}$$
$$- \frac{P^2}{4\pi \bar{E}_{\mathrm{PDMS}}} (3 - 2\gamma - 2 \ln kR), \qquad (6)$$

where the integration represents the work across the CNT/substrate interface. The minimization of Π_{tot} with respect to k and w_{max} gives

$$k \left(\frac{E_{\mathrm{CNT}}I}{\bar{E}_{\mathrm{PDMS}}} \right)^{1/4} = \left[\frac{2\pi(1 - \gamma - \ln kR)}{(3 - 2\gamma - 2 \ln kR)^2} \right]^{1/4}, \qquad (7)$$

$$w_{\mathrm{max}} = \frac{2}{k} \left[\varepsilon_{\mathrm{pre}} - \frac{E_{\mathrm{CNT}}I}{E_{\mathrm{CNT}}A} k^2 \right.$$
$$\left. - \frac{\pi \bar{E}_{\mathrm{PDMS}}}{E_{\mathrm{CNT}}Ak^2(3 - 2\gamma - 2 \ln kR)} \right]^{1/2}. \qquad (8)$$

Equation (7) is independent of the prestrain $\varepsilon_{\mathrm{pre}}$ and has the approximate solution (within a few percent error) for CNTs

$$k \approx \frac{3}{4} \left(\frac{\bar{E}_{\mathrm{PDMS}}}{E_{\mathrm{CNT}}I} \right)^{1/4}. \qquad (9)$$

The amplitude in Eq. (8) depends on the prestrain $\varepsilon_{\mathrm{pre}}$. From the vanishing amplitude $w_{\mathrm{max}} = 0$, we obtain the critical prestrain ε_c for the system to buckle
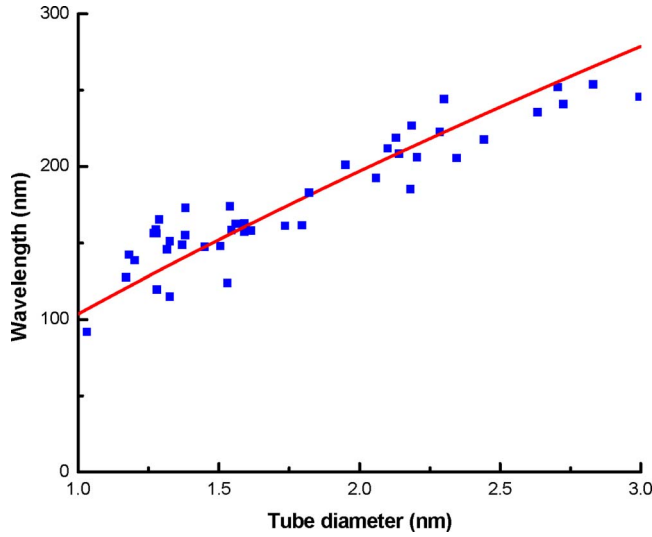
FIG. 2. (Color online) The wavelength of buckled single-walled CNTs on the PDMS substrate vs the tube diameter. The red line represents the theoretical prediction and blue dots are experimental data.

$$\varepsilon_c \approx \frac{16\sqrt{\bar{E}_{\mathrm{PDMS}}E_{\mathrm{CNT}}I}}{9E_{\mathrm{CNT}}A}\left(\frac{81}{256}\right.$$

$$\left. + \frac{2\pi}{6 - 4\gamma - 4\ln\dfrac{3}{4} - \ln\dfrac{\bar{E}_{\mathrm{PDMS}}R^4}{E_{\mathrm{CNT}}I}}\right). \tag{10}$$

A single-walled CNT can be modeled as a thin shell with thickness t. The bending and tensile stiffnesses become $(E_{\mathrm{CNT}}I)_{\mathrm{single}} = E_{\mathrm{CNT}}t \cdot \pi R^3$ and $(E_{\mathrm{CNT}}A)_{\mathrm{single}} = E_{\mathrm{CNT}}t \cdot 2\pi R$, respectively. Its Young's modulus and thickness always appear together via their product $E_{\mathrm{CNT}}t$. Therefore it is unnecessary to define Young's modulus and thickness separately since all experimentally measurable or theoretically calculable properties involve $E_{\mathrm{CNT}}t$, not E_{CNT} nor t separately.[30]

The wavelength for a single-walled CNT is obtained from Eq. (9) as

$$\lambda_{\mathrm{single}} = \frac{8\pi}{3}\left(\frac{E_{\mathrm{CNT}}t \cdot \pi R^3}{\bar{E}_{\mathrm{PDMS}}}\right)^{1/4}, \tag{11}$$

which is proportional to $R^{3/4}$. The above wavelength is shown versus the CNT radius R in Fig. 2 and is compared with the experimentally measured wavelength.[25] For the PDMS modulus $E_{\mathrm{PDMS}} = 2$ MPa, this gives $E_{\mathrm{CNT}}t = 0.42$ TPa nm, which is in the range of that reported by prior experiments and computations.[9–12,31–33]

III. BUCKLING OF MULTIWALLED CNTS

The above analysis for single-walled CNTs also holds for multiwalled CNTs and CNT bundles if $E_{\mathrm{CNT}}I$, $E_{\mathrm{CNT}}A$,
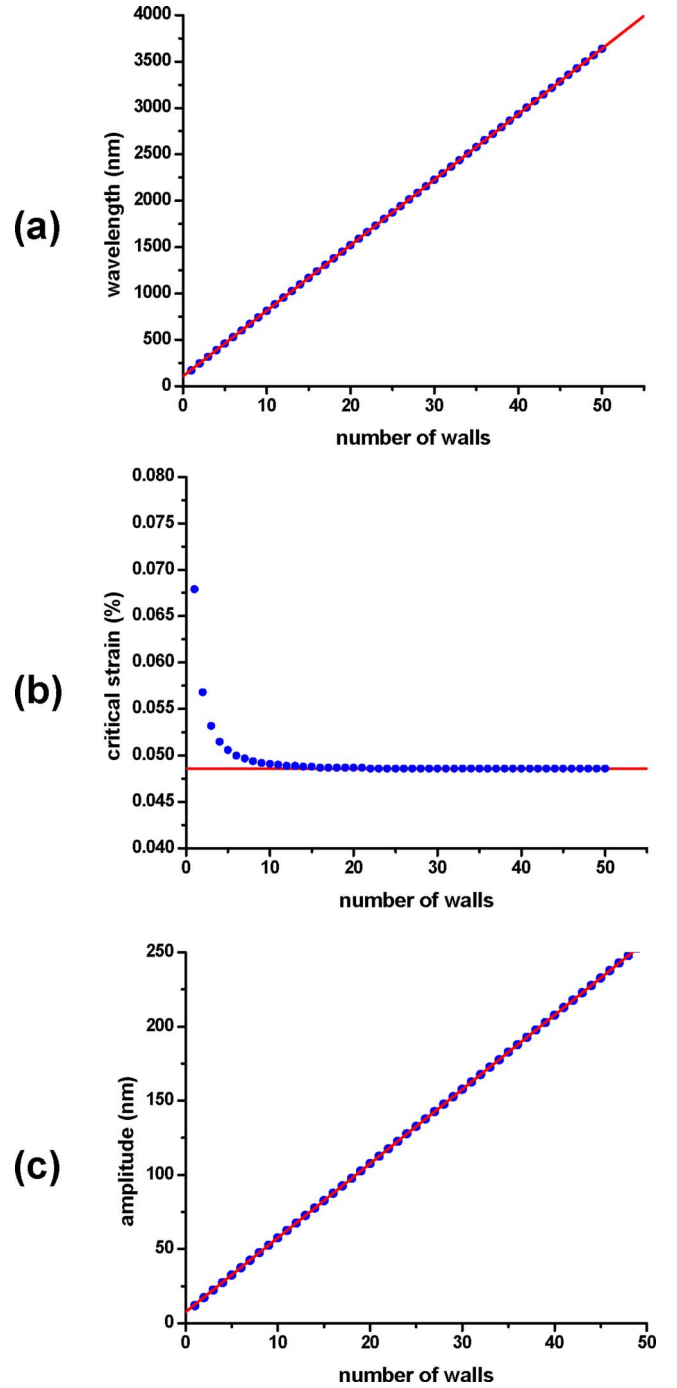

FIG. 3. (Color online) (a) The wavelength of buckled multiwalled CNTs increases linearly with the number of walls. The innermost wall is the (5, 5) armchair CNT with the radius 0.69 nm. The red line represents the approximation given by Eq. (13). (b) The critical strain for a multiwalled CNT to buckle vs the number of walls. The red line represents the asymptotic expression for critical strain given by Eq. (14). (c) The amplitude of a buckled multiwalled CNT increases linearly with the number of walls. The prestrain $\varepsilon_{\mathrm{pre}} = 5\%$. The red line represents the approximation given by Eq. (15).

and R are replaced with the corresponding bending stiffness, tension stiffness, and outer radius, respectively.

For a multiwalled CNT with the innermost wall radius R_{in}, n walls and interwall spacing $\sigma = 0.34$ nm, its bending stiffness $(E_{\mathrm{CNT}}I)_{\mathrm{multi}}$ is the sum of bending stiffness for all walls[34] and is given by[35]

$$(E_{CNT}I)_{multi} = (E_{CNT}I)_{in}n\left[1 + \frac{3(n-1)}{2}\frac{\sigma}{R_{in}}\right.$$
$$\left. + \frac{(n-1)(2n-1)}{2}\frac{\sigma^2}{R_{in}^2} + \frac{n(n-1)^2}{4}\frac{\sigma^3}{R_{in}^3}\right],$$
$$(12)$$

where $(E_{CNT}I)_{in} = E_{CNT}t \cdot \pi R_{in}^3$ is the bending stiffness of the innermost wall. Similarly, the tensile stiffness for a multiwalled CNT is $(E_{CNT}A)_{multi} = (E_{CNT}A)_{in}n[1+(n-1)/2(\sigma/R_{in})]$, where $(E_{CNT}A)_{in} = E_{CNT}t \cdot 2\pi R_{in}$ is the tensile stiffness of the innermost wall. Once again the bending and tensile stiffnesses depend on $E_{CNT}t$, not E_{CNT} or t separately.

The substitution of Eq. (12) into Eq. (11) gives the wavelength for a multiwalled CNT. It is shown versus the number of walls n in Fig. 3(a). The innermost wall is the (5, 5) armchair CNT with the radius 0.69 nm. For a large number of walls $n \gg 1$, as shown in Fig. 3(a), the wavelength can be approximated by

$$\lambda_{multi} \approx \frac{8\pi}{3}\left(\frac{E_{CNT}t \cdot \pi\sigma^3}{4\bar{E}_{PDMS}}\right)^{1/4}\left(n + \frac{R_{in}}{\sigma} - \frac{1}{2}\right), \qquad (13)$$

which increases linearly with the number of CNT walls. As shown in Fig. 3(a), the above expression is accurate for almost all n.

The critical buckle strain for multiwalled CNTs is approximately independent of the number of walls, as shown in Fig. 3(b). For $n \geq 5$, the critical strain is given by

$$\varepsilon_c \approx \frac{8}{9}\sqrt{\frac{\bar{E}_{PDMS}\sigma}{\pi E_{CNT}t}}\left(\frac{81}{256} + \frac{2\pi}{6 - 4\gamma - 2\ln\frac{9}{8} - \ln\frac{\bar{E}_{PDMS}\sigma}{\pi E_{CNT}t}}\right). \qquad (14)$$

The buckle amplitude of a multiwalled CNT is obtained by substituting Eq. (12) into Eq. (8), which is shown versus the number of walls in Fig. 3(c) for the prestrain $\varepsilon_{pre} = 5\%$. As shown in Fig. 3(c), the amplitude increases linearly with the number of walls for a large number of walls $n \gg 1$ and could be approximated by

$$w_{max} \approx \frac{8}{3}\left(n + \frac{R_{in}}{\sigma} - \frac{1}{2}\right)\left(\frac{E_{CNT}t \cdot \pi\sigma^3}{4\bar{E}_{PDMS}}\right)^{1/4}\left[\varepsilon_{pre} - \frac{8}{9}\sqrt{\frac{\bar{E}_{PDMS}\sigma}{\pi E_{CNT}t}}\left(\frac{81}{256} + \frac{2\pi}{6 - 4\gamma - 2\ln\frac{9}{8} - \ln\frac{\bar{E}_{PDMS}\sigma}{\pi E_{CNT}t}}\right)\right]^{1/2}. \qquad (15)$$

IV. BUCKLING OF CNT BUNDLES

For a representative CNT bundle of seven single-walled CNTs forming a hexagon,[36] as illustrated in Fig. 4(a), the bending stiffness is

$$(E_{CNT}I)_{bundle} = (E_{CNT}I)_{single}\left[7 + 6\left(2 + \frac{\sigma}{R}\right)^2\right], \qquad (16)$$

where $(E_{CNT}I)_{single} = E_{CNT}t \cdot \pi R^3$ is the bending stiffness of a single CNT with radius R and σ is the intertube spacing. The tensile stiffness for the CNT bundle is $(E_{CNT}A)_{bundle} = 7(E_{CNT}A)_{single}$. The wavelength, critical buckle strain, and amplitude of a buckled CNT bundle are shown versus the radius R of the constituent tube in Figs. 4(b)–4(d), respectively. The intertube spacing is 0.34 nm and the prestrain $\varepsilon_{pre} = 5\%$. For large tube radius $R \gg \sigma$, the wavelength, critical buckle strain, and amplitude of a buckled CNT bundle could be approximated by

$$\lambda_{bundle} \approx \frac{8\pi}{3}\left(\frac{31E_{CNT}t \cdot \pi R^3}{\bar{E}_{PDMS}}\right)^{1/4}\left(1 + \frac{6\sigma}{31R}\right), \qquad (17)$$

$$\varepsilon_c \approx \frac{8}{63}\sqrt{\frac{31\bar{E}_{PDMS}R}{\pi E_{CNT}t}}\left(1 + \frac{12\sigma}{31R}\right)$$
$$\times\left(\frac{81}{256} + \frac{2\pi}{6 - 4\gamma - 4\ln\frac{9}{2} - \frac{52\sigma}{93R} - \ln\frac{\bar{E}_{PDMS}R}{31\pi E_{CNT}t}}\right), \qquad (18)$$

$$w_{max} \approx \frac{8}{93}(31R + 6\sigma)\left(\frac{31\pi E_{CNT}t}{\bar{E}_{PDMS}R}\right)^{1/4}$$
$$\times\left[\varepsilon_{pre} - \frac{8}{63}\sqrt{\frac{31\bar{E}_{PDMS}R}{\pi E_{CNT}t}}\left(1 + \frac{12\sigma}{31R}\right)\left(\frac{81}{256}\right.\right.$$
$$\left.\left. + \frac{2\pi}{6 - 4\gamma - 4\ln\frac{9}{2} - \frac{52\sigma}{93R} - \ln\frac{\bar{E}_{PDMS}R}{31\pi E_{CNT}t}}\right)\right]^{1/2}. \qquad (19)$$

As shown in Fig. 4, the above expressions are rather accurate.

(a)
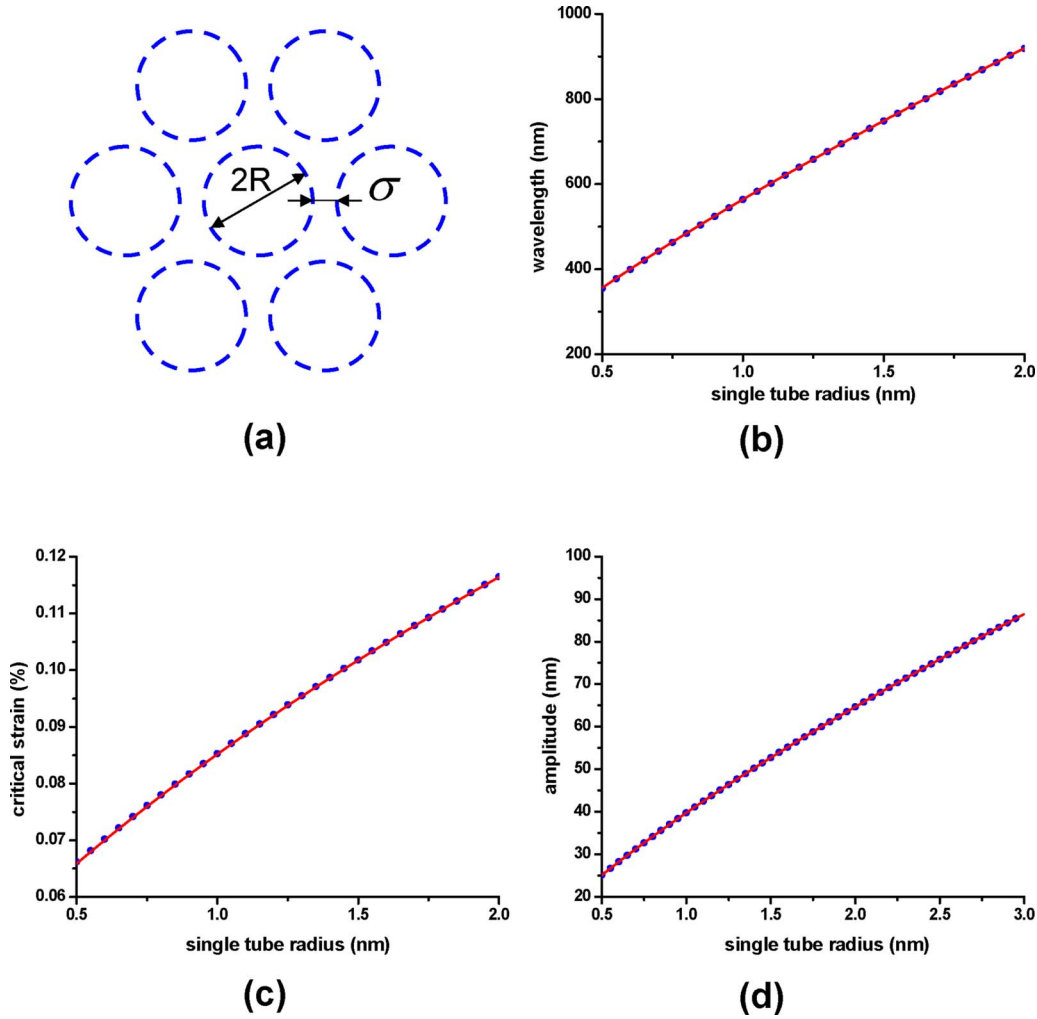

(b)

(c)

(d)

FIG. 4. (Color online) (a) A representative CNT bundle of seven single-walled CNTs forming a hexagon. The intertube spacing is 0.34 nm. (b) The wavelength of a buckled single-walled CNT bundle vs the radius of the constituent tube. The red line represents the approximation given by Eq. (17). (c) The critical strain for a single-walled CNT bundle to buckle vs the tube radius. The red line represents the approximation given by Eq. (18). (c) The amplitude of a buckled single-walled CNT bundle vs the tube radius. The red line represents the approximation given by Eq. (19).

V. COUPLED BUCKLING OF CNTS

The parallel CNTs buckle independently of the PDMS substrate when their spacing is large. Once their spacing decreases to a critical value, the CNTs interact via the substrate and buckle together and therefore have the same wavelength and phase. For two parallel CNTs with outermost wall radii R_j, bending stiffness $E_{CNT}I_j$, tensile stiffness $E_{CNT}A_j$ ($j = 1, 2$), and center to center spacing $2d$ to buckle together, the out-of-plane displacements can be written as $w_j = w_{\max j} \cos kx$, with the wave number k and amplitudes $w_{\max j}$ to be determined. The bending and membrane energies in two CNTs are still given by Eqs. (1) and (2) with the bending stiffness, tensile stiffness, and amplitude replaced by $E_{CNT}I_j$, $E_{CNT}A_j$, and $w_{\max j}$, respectively. The magnitude P of normal traction at the CNT/substrate interface is replaced by $P_j = E_{CNT}A_j k^2 w_{\max j}(\varepsilon_{pre} - k^2 w_{\max j}^2/4) - E_{CNT}I_j k^4 w_{\max j}$.

The PDMS substrate is subjected to two normal surface tractions $P_1 \cos kx/(2R_1)$ and $P_2 \cos kx/(2R_2)$ over the widths $2R_1$ and $2R_2$, respectively. The strain energy in the substrate is obtained as

$$U_{PDMS} = \frac{P_1^2}{4\pi \bar{E}_{PDMS}}(3 - 2\gamma - 2\ln kR_1)$$
$$+ \frac{P_2^2}{4\pi \bar{E}_{PDMS}}(3 - 2\gamma - 2\ln kR_2) + \frac{P_1 P_2}{2\pi \bar{E}_{PDMS}}f(k),$$

$$(20)$$

where

$$f(k) = (3 + 2\ln 2 - 2\gamma) + k^2 d^2\left(\frac{19}{6} + 2\ln 2 - 2\gamma\right)$$

$$+ \frac{1}{96R_1 R_2}\{[24 + k^2(2d + R_1 - R_2)^2](2d + R_1$$

$$- R_2)^2 \ln[k(2d + R_1 - R_2)] + [24 + k^2(2d - R_1$$

$$+ R_2)^2](2d - R_1 + R_2)^2 \ln[k(2d - R_1 + R_2)] - [24$$

$$+ k^2(2d - R_1 - R_2)^2](2d - R_1 - R_2)^2 \ln[k(2d - R_1$$

$$- R_2)] - [24 + k^2(2d + R_1 + R_2)^2](2d + R_1$$

$$+ R_2)^2 \ln[k(2d + R_1 + R_2)]\} \tag{21}$$

results from the interactions.

The total potential energy Π_{tot} of the system is

$$\Pi_{\text{tot}} = \frac{1}{4}\sum_{j=1}^{2}\left[E_{\text{CNT}}I_j k^4 w_{\max j}^2 + 2E_{\text{CNT}}A_j\left(\frac{1}{4}k^2 w_{\max j}^2 - \varepsilon_{\text{pre}}\right)^2 \right.$$
$$\left. + 2P_j w_{\max j} - \frac{P_j^2}{\pi\bar{E}_{\text{PDMS}}}(3 - 2\gamma - 2\ln kR_j) \right]$$
$$- \frac{P_1 P_2}{2\pi\bar{E}_{\text{PDMS}}}f(k). \tag{22}$$

Its minimization gives the wave number k and amplitudes $w_{\max 1}$ and $w_{\max 2}$. For two double-walled CNTs with inner wall radii 1 and 1.1 nm (which correspond to the outer wall radii $R_1 = 1.34$ nm and $R_2 = 1.44$ nm, respectively) to buckle together, Fig. 5(a) shows the total potential energy of the system versus the wall-to-wall spacing $2d - R_1 - R_2$ between two CNTs. For comparison, the potential energy for them to buckle independently is also shown by the horizontal line. The curve and the horizontal line intersect and give a critical distance, 84 nm, below which the double-walled CNTs buckle together on the PDMS substrate. As shown in Fig. 5(b), this critical distance for two double-walled CNTs to buckle together decreases as the difference in CNT radii increases, which suggests that CNTs with the same radii are easier to buckle together than those with different radii. Figure 5(c) compares the wavelength of coupled buckling to the wavelengths of two independently buckled double-walled CNTs. It is clear that the larger tube dominates the coupled buckling since the wavelength is close to that of the larger tube.

VI. CONCLUSION

The buckling of single-walled, multiwalled CNTs, and CNT bundles on the elastomeric substrate is studied via the continuum mechanics theory. Simple expressions of the buckle wavelength and amplitude and the critical strain for buckling are obtained analytically. For single-walled CNTs, the wavelength is proportional to the CNT radius to the 3/4 power, while it increases linearly with the number of walls for multiwalled CNTs. For two parallel CNTs on the surface of the elastomeric substrate, there exists a critical spacing below which the two CNTs interact and buckle together, adopting the same wavelength. This cobuckling wavelength is very close to the wavelength for the larger CNT to buckle independently, i.e., the larger tube dominates the coupled buckling.
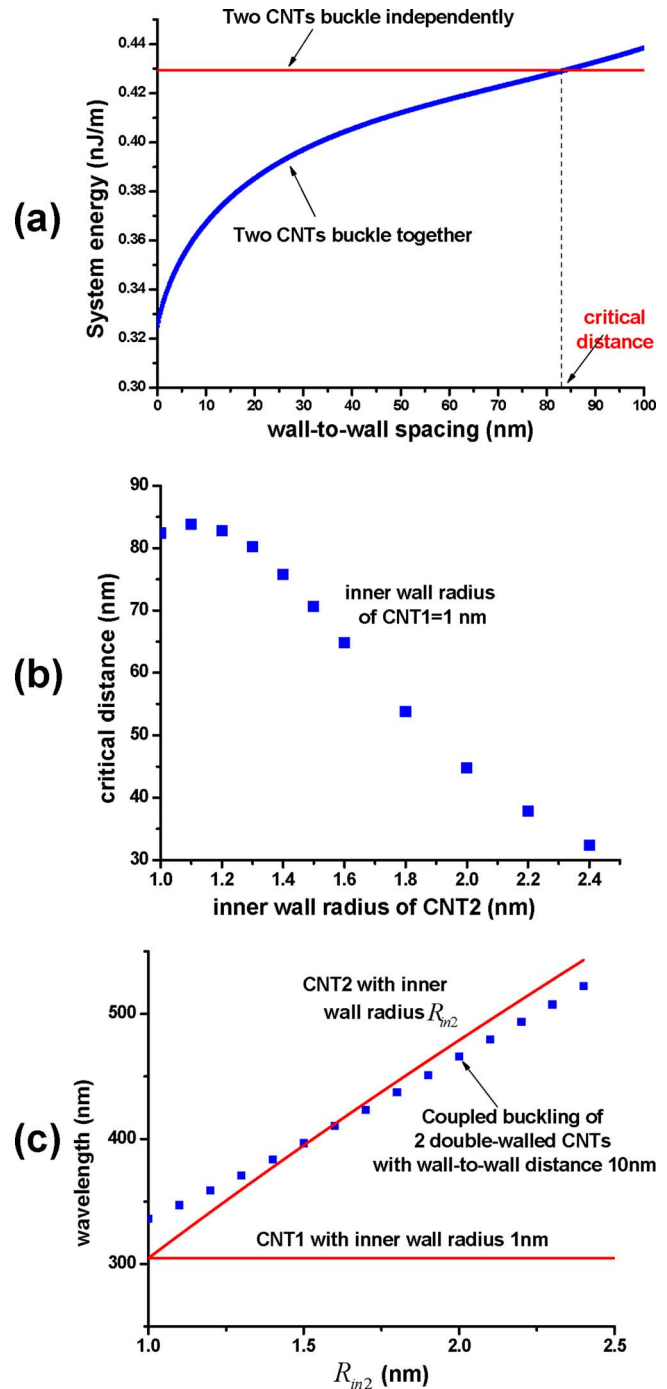
ACKNOWLEDGMENTS

FIG. 5. (Color online) (a) The total potential energy of two double-walled CNTs with inner wall radii 1 and 1.1 nm buckled together. The red horizontal line is the total energy for them to buckle independently. The curve and the horizontal line intersect and give a critical distance, 84 nm, below which the CNTs buckle together on the PDMS substrate. (b) The critical distance for two CNTs to buckle together decreases as the difference in CNT radii increases. (c) The wavelength of coupled buckling (blue dots) vs the wavelengths of two independently buckled double-walled CNTs (red lines). It is clear that the larger tube dominates the coupled buckling since the wavelength is close to that of the larger tube.

[1] Y. Sun and J. A. Rogers, J. Mater. Chem. **17**, 832 (2007).
[2] Y. Sun, W. M. Choi, H. Jiang, Y. Y. Huang, and J. A. Rogers, Nat. Nanotechnol. **1**, 201 (2006).
[3] Y. Sun, V. Kumar, I. Adesida, and J. A. Rogers, Adv. Mater. (Weinheim, Ger.) **18**, 2857 (2006).
[4] V. J. Lumelsky, M. S. Shur, and S. Wagner, IEEE Sens. J. **1**, 41 (2001).
[5] D. Y. Khang, H. Q. Jiang, Y. Huang, and J. A. Rogers, Science **311**, 208 (2006).
[6] S. P. Lacour, J. Jones, S. Wagner, T. Li, and Z. Suo, Proc. IEEE **93**, 1459 (2005).
[7] C. M. Stafford, C. Harrison, K. L. Beers, A. Karim, E. J. Amis, M. R. VanLandingham, H.-C. Kim, W. Volksen, R. D. Miller, and E. E. Simonyi, Nat. Mater. **3**, 545 (2004).
[8] A. J. Nolte, M. F. Rubner, and R. E. Cohen, Macromolecules **38**, 5367 (2005).
[9] B. I. Yakobson, C. J. Brabec, and J. Bernholc, Phys. Rev. Lett. **76**, 2511 (1996).
[10] M. F. Yu, O. Lourie, M. J. Dyer, K. Moloni, T. F. Kelly, and R. S. Ruoff, Science **287**, 637 (2000).
[11] M. M. J. Treacy, T. W. Ebbesen, and J. M. Gibson, Nature (London) **381**, 678 (1996).
[12] T. W. Tombler, C. W. Zhou, L. Alexseyev, J. Kong, H. J. Dai, L. Lei, C. S. Jayanthi, M. J. Tang, and S. Y. Wu, Nature (London) **405**, 769 (2000).
[13] P. Poncharal, Z. L. Wang, D. Ugarte, and W. A. de Heer, Science **283**, 1513 (1999).
[14] J. Xiao, B. Liu, Y. Huang, J. Zuo, K. C. Hwang, and M. F. Yu, Nanotechnology **18**, 395703 (2007).
[15] M. F. Yu, T. Kowalewski, and R. S. Ruoff, Phys. Rev. Lett. **86**, 87 (2001).
[16] Z. L. Wang, P. Poncharal, and W. A. de Heerb, J. Phys. Chem. Solids **61**, 1025 (2000).
[17] R. Martel, V. Derycke, C. Lavoie, J. Appenzeller, K. K. Chan, J. Tersoff, and Ph. Avouris, Phys. Rev. Lett. **87**, 256805 (2001).
[18] A. Bezryadin, A. R. M. Verschueren, S. J. Tans, and C. Dekker, Phys. Rev. Lett. **80**, 4036 (1998).
[19] S. Paulson, M. R. Falvo, N. Snider, A. Helser, T. Hudson, A. Seeger, R. M. Taylor, R. Superfine, and S. Washburn, Appl. Phys. Lett. **75**, 2936 (1999).
[20] B. B. Liu, B. Sundqvist, O. Ansersson, T. Wagberg, E. B. Nyeanchi, X. M. Zhu, and G. T. Zou, Solid State Commun. **118**, 31 (2001).
[21] X. Zhou, J. J. Zhou, and Z. C. Ou-Yang, Phys. Rev. B **62**, 13692 (2000).
[22] E. Artukovic, M. Kaempgen, D. S. Hecht, S. Roth, and G. Grüner, Nano Lett. **5**, 757 (2005).
[23] H. Maune and M. Bockratha, Appl. Phys. Lett. **89**, 173131 (2006).
[24] C. Kocabas, H.-S. Kim, T. Banks, J. A. Rogers, A. A. Pesetski, J. E. Baumgardner, S. V. Krishnaswamy, and H. Zhang, Proc. Natl. Acad. Sci. U.S.A. **105**, 1405 (2008).
[25] D. Y. Khang, J. Xiao, C. Kocabas, S. MacLaren, T. Banks, H. Jiang, Y. Y. Huang, and J. A. Rogers, Nano Lett. **8**, 124 (2008).
[26] Z. Y. Huang, W. Hong, and Z. Suo, J. Mech. Phys. Solids **53**, 2101 (2005).
[27] S. P. Timoshenko, *Strength of Materials*, 3rd ed. (Van Nostrand, New York, 1956).
[28] S. P. Timoshenko and J. N. Goodier, *Theory of Elasticity*, 3rd ed. (McGraw-Hill, New York, 1970).
[29] D. Armani, C. Liu, and N. Aluru, Proceedings of IEEE Micro Electro Mechanical System (MEMS) '99, Orlando, FL, 17–21 January 1999 (IEEE, Piscataway, NJ, 1999), pp. 222–227.
[30] J. Wu, K. C. Hwang, and Y. Huang, J. Mech. Phys. Solids **56**, 279 (2008).
[31] E. W. Wong, P. E. Sheehan, and C. M. Lieber, Science **277**, 1971 (1997).
[32] J. P. Lu, Phys. Rev. Lett. **79**, 1297 (1997).
[33] G. Van Lier, C. V. Alsenoy, V. V. Doran, and P. Geerlings, Chem. Phys. Lett. **326**, 181 (2000).
[34] A. Pantano, M. C. Boyce, and D. M. Parks, Phys. Rev. Lett. **91**, 145504 (2003).
[35] W. Zhou, Y. Huang, B. Liu, K. C. Hwang, J. M. Zuo, M. J. Buehler, and H. Gao, Appl. Phys. Lett. **90**, 073107 (2007).
[36] D. Qian, W. K. Liu, and R. S. Ruoff, Compos. Sci. Technol. **63**, 1561 (2003).